Comparing Gluon to Quark Jets with Delphi

Oliver Klapp, Patrick Langefeld

Univ. Wuppertal, FB 8, Gaußstr. 20, 42097 Wuppertal, Germany

Delphi *Collaboration*

E-mail: Klapp@WHEP.uni-wuppertal.de

This is a summary of the latest results of the Delphi Collaboration on the properties of identified quark and gluon jets. It covers the measurement of the fragmentation functions of gluons and quarks and their scaling violation behaviour as well as an analysis of the scale dependence of the multiplicities in gluon and quark jets. Further, a precision measurement of C_A/C_F from the multiplicities in symmetric three jet events is discussed.

I. INTRODUCTION

In QCD, the three fundamental splittings of the two types of colour charged fields participating in the strong interaction (quarks (q) and gluons (g)) are $q \to qg$, $g \to gg$, and $g \to q\bar{q}$. The corresponding *splitting kernels*, which describe both the kinematics and the relative strengths of these splittings, are proportional to the *colour factors* $C_F = \frac{4}{3}, C_A = 3$, and $T_R = \frac{1}{2}n_F$, respectively, where n_F is the number of active quark flavours in $g \to q\bar{q}$ decays. The values for these colour factors originate directly from the group $\mathcal{SU}(3)$ underlying QCD so that precise measurements of these couplings validate QCD as the fundamental theory for strong interactions. In the sensible range of $n_F = 3 \ldots 5$, the ratio of the splitting kernels $S_{(g \to gg + g \to q\bar{q})}/S_{(q \to qg)}$ is nearly constant (2.0 - 2.3) and exactly $C_A/C_F =$2.25 in limit of large energy transfers. This leads to the expectation of a C_A/C_F times higher probability of gluon bremsstrahlung in gluon jets with respect to quark jets. This ratio should be visible for observables which are proportional to the splitting probabilities of gluons and quarks [1].

Unfortunately, quarks and gluons are no free particles. Therefore one has to use jets of gluons and quarks in three jet events as the best approximation of the tree level graphs. Beyond the necessity to rely on the assumption of LPHD (**L**ocal **H**adron **P**arton **D**uality) which states that the parton properties are preserved to the hadron level which is then clustered to jets, this approach is further limited by the influence of interference effects in the event. Moreover the assignment of particles to jets is somewhat arbitrarily.

Further, the jet finding algorithms introduce ambiguities when assigning particles to jets.

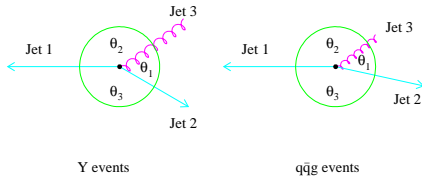## II. EXPERIMENTAL ACCESS TO GLUON AND QUARK JETS

FIG. 1. Symmetric and asymmetric event topologies

Gluon jets were originally identified in symmetric three jet events (Y *events*) [2–4]. In these events the most energetic jet is excluded from the analysis, as the rate of gluon induced leading jets is rather low. Due to the symmetric event topology ($\theta_2 \sim \theta_3$, see Fig. 1), the low energy jets are expected to be directly comparable. By identifying one of these jets as a b-quark jet using impact parameter techniques, the remaining jet is identified indirectly as a gluon jet. The properties of a comparable *udsc*-quark jet sample can then be obtained from non-b events, where the gluon properties are eliminated from by subtraction techniques [3,4].

Recently this technique has also been extended to non-symmetric events [4] (see Fig. 1). In this case one relies on the quark/gluon composition of jets as predicted by the three jet matrix elements taken from Monte Carlo simulations. This technique improves the available statistic and gives access to a wider range of energy scales, but requires a criterion for the selection of comparable gluon and quark jets. These jets are obtained from events with different topologies.

The comparison of jet properties obtained for this event sample[1] and for Y events helps in finding a suitable scale to classify the jets with. One yields about 20,000 identified gluons in Y events and about 100,000 in the asymmetric events.

III. JET SCALES

The relevant scale for the jet evolution is not just the jet energy. In FIG. 2, the fragmentation functions of quark jets as a function of their energy are shown. The *rows* in this figure correspond to data taken in the same x_E intervals. The much more pronounced scaling violation pattern of jets obtained from symmetric events ($E_{Jet} \sim 22 GeV \ldots 29 GeV$) compared to jets from asymmetric events clearly disfavours the jet energy as the relevant scale.

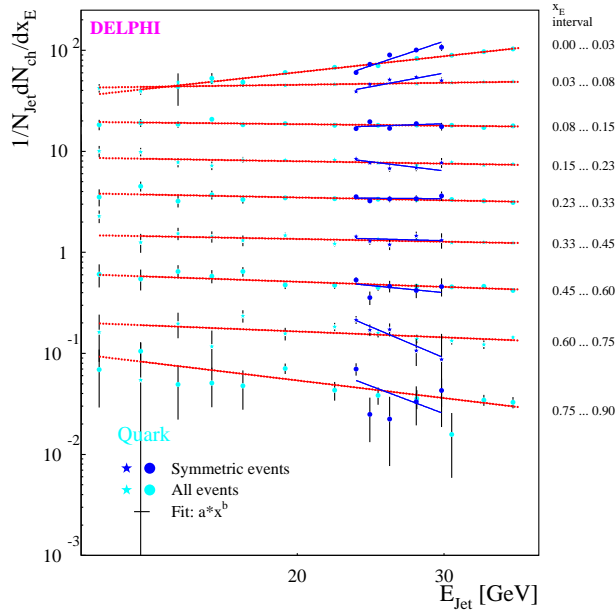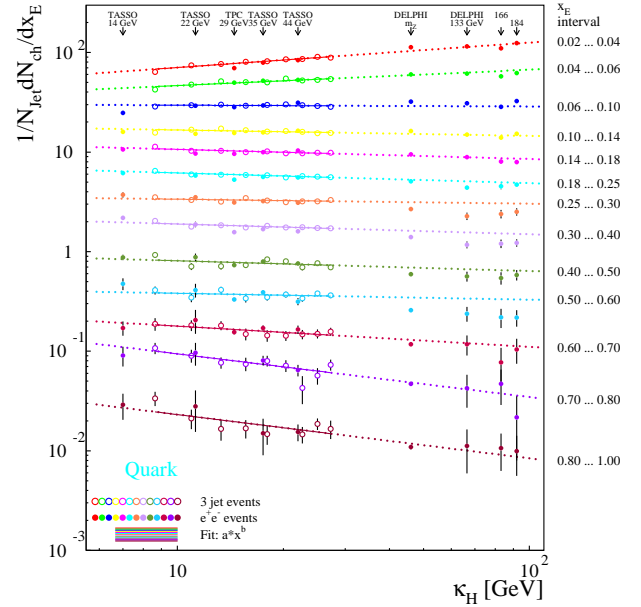FIG. 2. Quark frag. func. vs. E_{Jet}.

FIG. 3. Quark frag. func. vs. κ_H

Soft radiation is limited to cones given by the opening angles between the jets. This motivates transverse momentum scales. The *hardness* $\kappa_H = E \sin \theta_1 / 2$ is a better choice [8], as it accounts for the limited phase space available for gluon radiation due to the interference of radiated gluons in the event[2]. FIG. 3 shows the good agreement of light quark jets in three jet events with jets in e^+e^- annihilations from PETRA energies [9] to the highest LEP energies [10] in normalization and slopes using κ_H for the first and E_{beam} for the latter. This agreement confirms the interpretation of κ_H as a valid scale for jet evolution in three jet events. In multi-jet events several scales may be relevant; in so far the usage of κ_H as a (single) scale is an approximation. Another possible choice is the scale p_1^T, introduced in SEC. IV D.

IV. RESULTS

Recently, several properties of quark and gluon jets which can be expected to be sensitive to C_A / C_F, such as the scaling violation of quark and gluon jets [11] and the scale dependence of the quark and gluon jet multiplicities [12] have been analysed using data collected with the DELPHI detector at LEP.

---

[1] In the following called *asymmetric* event sample though containing all Y events as well.
[2] This definition corresponds to the **beam** energy of an $e^+e^- \to q\bar{q}$ event. Often also the definition $\kappa = 2E \sin \theta/2 \sim E\theta$ is used.

A. Gluon and Quark Fragmentation Functions

The gluon and quark fragmentation functions $D_{g,q}(x_E, \kappa_H)$ are measured in dependence of different values of κ_H at a fixed CMS energy (see SEC. III for a short discussion of jet scales).
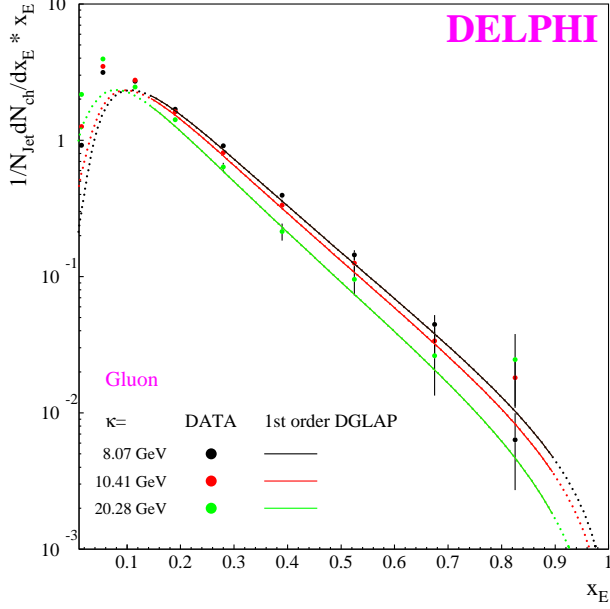

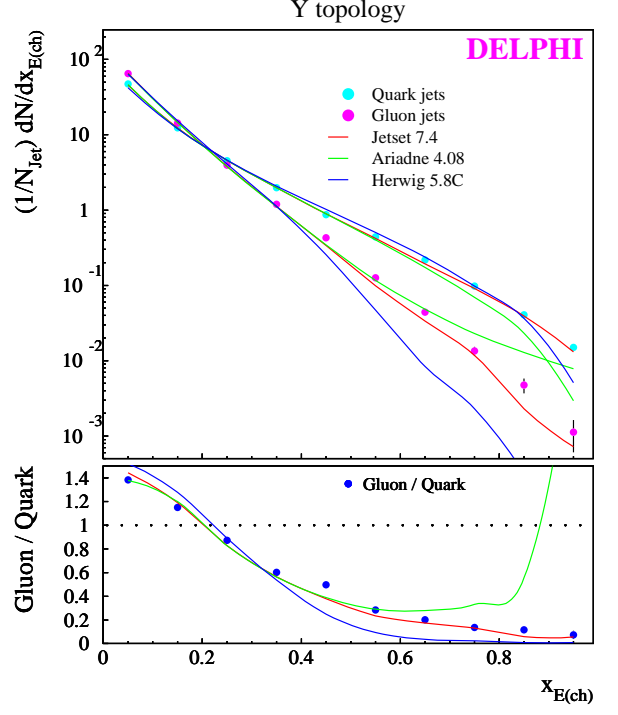FIG. 4. Gluon fragmentation functions for different values of κ_H

FIG. 5. Gluon and quark fragmentation function at a fixed topology, $\theta_2, \theta_3 \in [150° \pm 15°]$), compared to different Monte CArlo generators

The predictions are derived from the numerical solution of the DGLAP evolution equation in first order [5]. The following ansatz has been used to parameterize the fragmentation function at a fixed scale κ_0 to start the evolution:

$$D_p^{g,q}(x_E) = p_3^{g,q} \cdot x_E^{p_1^{g,q}} \cdot (1 - x_E)^{p_2^{g,q}} \cdot \exp\left(-p_4^{g,q} \cdot \ln^2 x_E\right). \tag{1}$$

The parameters $p_i^{q,g}$, Λ_{QCD} and the colour factor C_A are fitted simultaneously.

The softening of the fragmentation functions with increasing κ is observed. This effect is more pronounced for gluon jets than for quark jets. Fig. 5 compares the gluon and the quark fragmentation function at a fixed topology.

B. Scaling violation of the gluon and quark fragmentation functions

FIG. 3 shows the measurement for light quark jets in three jet events as a function of κ_H, represented by the open symbols and superimposed by power law fits. The corresponding result for gluons is shown in FIG. 6 for symmetric and asymmetric event topologies. The good agreement between the two event samples in FIG. 6 demonstrates that κ_H is a sensible choice for the scale of gluon jets as well.

A simultaneous fit with the first order DGLAP equations to both the quark and gluon fragmentation functions has been performed. Beyond the parameters of the analytic ansatz of the fragmentation functions , Λ_{QCD} and C_A have been treated as free parameters. The fit is sensitive to the occurrence of C_A in the $g \to gg$ splitting kernel. The fit describes the data well and yields:
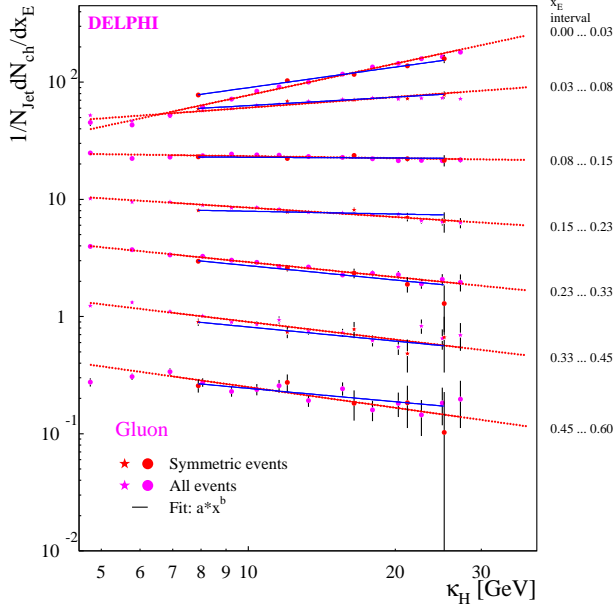
FIG. 6. Gluon fragmentation functions as a function of jet scale κ_H. Superimposed are jets from both symmetric and asymmetric events
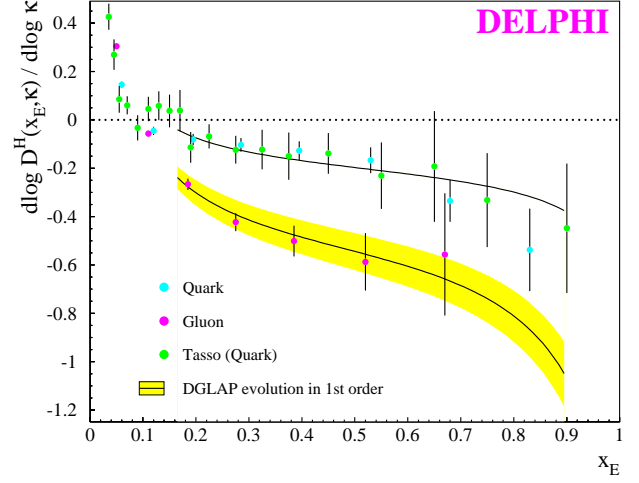

FIG. 7. (Logarithmic) slopes of the scale (κ_H) dependence of the quark and gluon fragmentation functions as a function of x_E

$$\frac{C_A}{C_F} = 2.44 \pm 0.21_{stat}(\text{preliminary}).$$

for the colour factor ratio.

In FIG. 7 the logarithmic slope of the gluon and quark fragmentation functions are compared in dependence of x_E superimposed by the result of the DGLAP fits. The shaded area indicates the statistical uncertainty of C_A. The data points were obtained from power law fits to each x_E interval individually. As expected from the structure of the DGLAP equation, the scaling violations are ~ 2 times larger for gluons than for quarks. Furthermore, the observed scaling violation in quark jets is in very good agreement with the measurements of the TASSO Collaboration [9] (already visible in FIG. 3).

C. Scale dependence of the gluon and quark jet multiplicities

There is a long standing QCD prediction that in the limit of large parton (or jet) energies the ratio $r_n = \langle N_g \rangle / \langle N_q \rangle$ of the gluon over the quark multiplicity should be equal to C_A/C_F [1]. Following a NNLO calculation [13], r_n is reduced by $\sim 10\%$ and nearly independent of energy. FIG. 8 shows the scale dependence of the jet multiplicity and FIG. 9 shows this ratio as a function of the hardness κ_H. Obviously, the ratio is much lower than expected; consequently neither the LO nor the NNLO prediction for r_n can describe the measured data.

To describe the quark and gluon jet multiplicities, one would set $\langle N_q \rangle = \langle N_{pert} \rangle$ as calculated from some QCD approach [14,15] and $\langle N_g \rangle = r_n \cdot \langle N_{pert} \rangle$, with $r(\kappa_H) = C_A/C_F[1 - r_1\gamma_0(\alpha_S) - r_2\gamma_0^2(\alpha_S)]$. A modification of this ansatz had to be performed to obtain a sensible description of the measured data:

$$\langle N_q \rangle(\kappa_H) = \langle N_{pert} \rangle(\kappa_H) + N_0^q \tag{2}$$

$$\langle N_g \rangle(\kappa_H) = \langle N_{pert} \rangle(\kappa_H) \cdot r_n + N_0^g \tag{3}$$

The introduction of the phenomenological offsets N_0^q and N_0^g which are assumed to be constant, accounts for expected differences of the fragmentation of the leading quark or gluon.
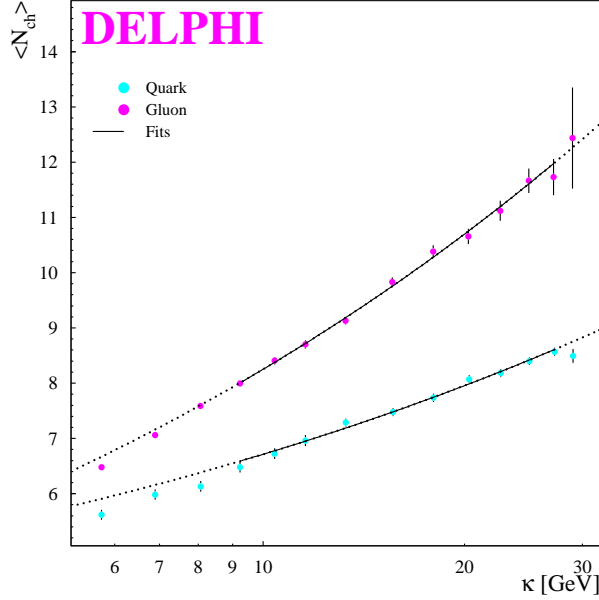
4

FIG. 8. Average charged multiplicity for light quark and gluon jets as a function of κ_H fitted with Eqn.2 and 3
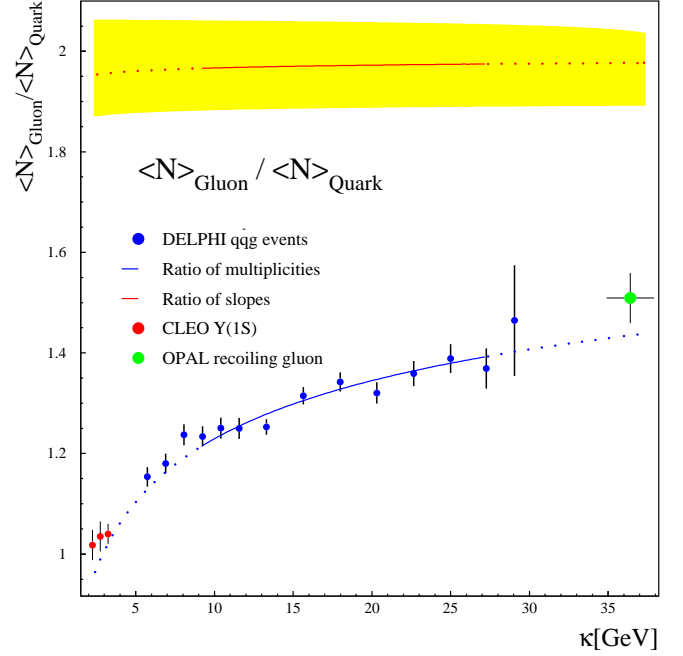

FIG. 9. Ratio of gluon and quark jet multiplicities and their slopes as a function of κ_H

The quality of the fit increases from χ^2/ndf=14.5 to 0.85 when introducing these additional terms. The difference N_0^q-N_0^g yields about 2, consistent with about one additional *instable* primary particle built in the primary quark fragmentation. Unlike the multiplicity ratio itself, the ratio of derivatives of the gluon and quark multiplicities with scale $\partial\langle N_g\rangle(\kappa_H)/\partial\kappa_H \,/\, \partial\langle N_q\rangle(\kappa_H)/\partial\kappa_H$ is in the predicted range of ~ 2 already at very small scale values (see FIG. 9). This corresponds to the expectation that if the multiplicity ratio is C_A/C_F in the limit of very large energies, the ratio of the slopes shows the same behaviour, simply due to de l'Hôpital's rule. There should be less sensitivity of the slope ratio to non-perturbative effects than of the multiplicity ratio itself. Furthermore, the fit to the quark and gluon jet multiplicities extrapolates very well to the multiplicity ratios measured by CLEO (direct measurement of $e^+e^- \to \Upsilon(1s) \to gg\gamma$ decays) [6] and OPAL (analysis of most energetic jets) [7], which is a confirmation of this analysis.

Fitting EQ. 2 and 3 to the data yields $C_A/C_F = 2.12 \pm 0.10_{stat}$, in agreement with QCD. Nevertheless, large systematic errors are here to be expected for this value due to ambiguities in the assignment of particles to jets, the definition of the three jet region and the choice of the underlying jet scale.

D. Measurement of C_A/C_F from three jet event multiplicities

The uncertainties in the determination of the colour factor ratio quoted in SEC. IV C can be avoided by applying a MLLA prediction [8] for three jet event multiplicities, $N_{q\bar{q}g}$, to the data:

$$N_{q\bar{q}g} = N_{e^+e^-}(2E^*) + r_n(p_1^T) \cdot \left\{ \frac{1}{2} \cdot N_{e^+e^-}(p_1^T) - N_0 \right\} \tag{4}$$

$$\text{with}: \quad p_1^T = \sqrt{2\frac{(p_q p_g)(p_{\bar{q}} p_g)}{p_q p_{\bar{q}}}} \quad ; \quad 2E^* = \sqrt{2p_q p_{\bar{q}}} \quad ; \quad p_i : \text{four} - \text{momenta}$$

The first term represents the multiplicity of an e^+e^- event at a CMS energy of the invariant mass of the $q\bar{q}$ system, the second term half the multiplicity of a hypothetical $e^+e^- \to gg$ event with a CMS energy of twice the transverse momentum of the gluon. Coherence effects are included by the exact definition of the scales. Again, the term "-N_0" was introduced into the original MLLA prediction to absorb non-perturbative contributions.

Eq. 4 has been applied to strictly symmetric events with $\theta_2, \theta_3 = (\pi - \theta_1/2) \pm 1.5°$. Therefore the only parameter describing the event topology is the opening angle θ_1. $N_{e^+e^-}(\sqrt{s})$ has been chosen as $N_{pert}(\sqrt{s})$ [14,15] (as in Sec. IV C); the free parameters of these formulae are obtained from the multiplicities of e^+e^- events as a function of the CMS energy. Fig. 8 shows the three jet event multiplicities as a function of the opening angle θ_1. Superimposed is the fit with C_A/C_F and N_0 as free parameters as a solid line, extrapolated to the region contaminated by two jet events ($\theta_1 < 35°$), which is excluded from the fit. The dashed line represents the original prediction ($C_A/C_F = 2.25$, and $N_0 = 0$). The need for some kind of correction to account for non-perturbative effects is obvious, and the ansatz of adding a constant term is a simple but effective choice. The fit yields a very precise accurate measurement of C_A/C_F :

$$\frac{C_A}{C_F} = 2.246 \pm 0.062_{stat} \pm 0.080_{sys} \pm 0.095_{theo} . \tag{5}$$
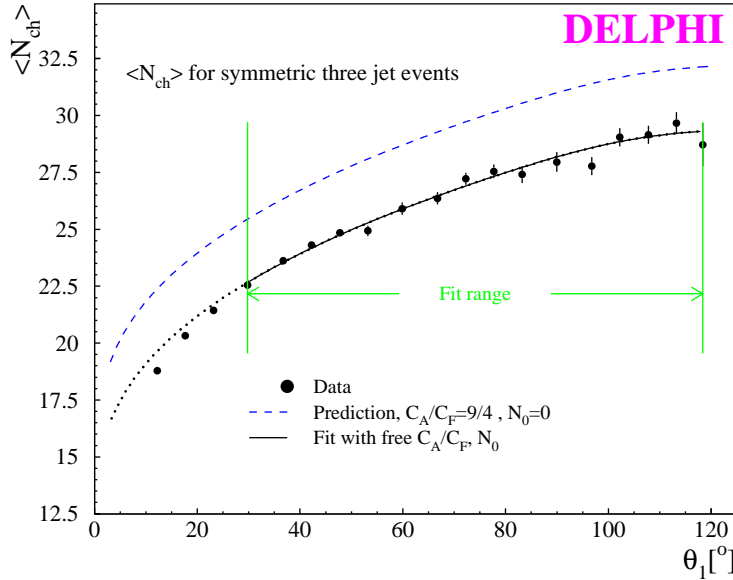

FIG. 9. Three jet event multiplicities

The prediction of the multiplicity ratio given in [16] has been tried as an alternative to the given r_n. Although this calculation takes recoil effects into account, a non-perturbative offset term is still required. The prediction differs by about 10% from [13] in the NNLO term. As it does not reproduce the colour factor ratio contained in the fragmentation models which describe the data well, it has not been applied in this analysis. Fig. 10 shows the obtained result for the colour factor ratio in comparison of those obtained from four jet analyses. As far as we know our result is the most accurate measurement of C_A/C_F so far.

In order to illustrate comprehensively the contents of the measurement of the three jet multiplicity we compare in Fig. 11 the multiplicity corresponding to a gg and a $q\bar{q}$ final state. The $q\bar{q}$ multiplicity is taken to be the multiplicity measured in e^+e^- annihilation corrected for the $b\bar{b}$ contribution. The gg multiplicity at low scale values is taken from the CLEO measurement [6], for which no systematic error was specified. At higher scale, twice the difference of the three jet multiplicity and the $q\bar{q}$ term (the first term in Eqn. 4) is interpreted as the gg multiplicity. The dashed curve through the $q\bar{q}$ points is a fit of $N_{pert}(\sqrt{S})$. The gg line is the perturbative expectation for back-to-back gluons according to the second term of Eqn. 4. The plot shows again that the increase of the gg multiplicity with scale is about twice as big as in the $q\bar{q}$ case, illustrating the large gluon-to-quark colour factor ratio C_A/C_F .
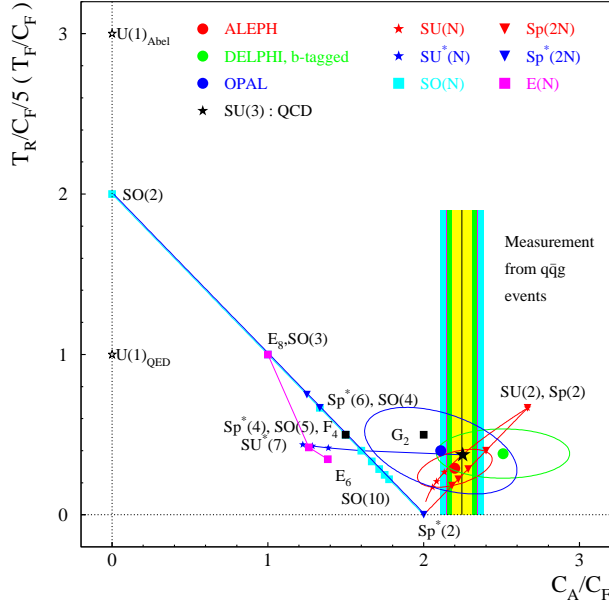
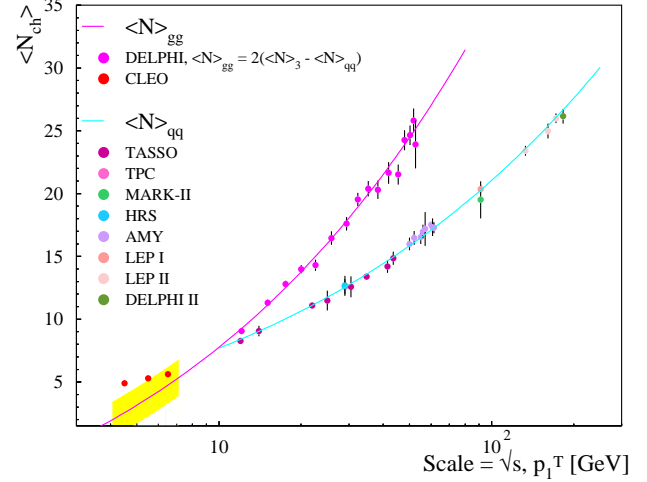## ACKNOWLEDGMENTS

FIG. 10. The colour factor group plot

FIG. 11. Comparison of the charged hadron multiplicity for an initial $q\bar{q}$ and a gg pair as function of the scale. The dashed curve is a fit according of $N_{pert}(\sqrt{S})$, the full line is twice the second term of Eqn. 4. The shaded band indicates the uncertainty due to the error of N_0.

[1] S.J. Brodsky and J.F. Gunion, *Phys. Rev. Lett.* **37**, 402 (1976);
K. Konishi et al., *Phys. Rev. Lett.* **78**, 243 (1978).
[2] DELPHI Coll., *Z. Phys.* C **70**, 179 (1996);
[3] O. Klapp, Diplomarbeit, Bergische Univ. - GH Wuppertal, WUD 95-15.
[4] M. Siebel, Diplomarbeit, Bergische Univ. - GH Wuppertal, WUD 97-43.
[5] V.N. Gribov, L.N. Lipatov, *Sov. J. Nucl. Phys.* **15**, 438 and 675 (1972).
G. Altarelli, G. Parisi, *Nucl. Phys.* B **126**, 298 (1977);
Yu.L. Dokshitzer, *Sov. Phys. JETP* **46**, 641 (1977).
[6] CLEO Coll., *Phys. Rev.* D **56**, 17 (1997).
[7] OPAL Coll., *Eur. Phys. J.* C **1**, 479 (1998).
[8] V. A. Khoze and W. Ochs, *Int. J. Mod. Phys.* A **12**, 2949 (1997).
[9] TASSO Coll., *Z. Phys.* C **45**, 193 (1989).
[10] DELPHI Coll., Contr. Paper 138 to the XXIX ICHEP, Vancouver, 1998.
[11] K.Hamacher, O.Klapp, P.Langefeld, M.Siebel et al.
Scaling Violations of Quark and Gluon Fragmentation Functions,
Contr. Paper 147 to the XXIX ICHEP, Vancouver, 1998.
[12] DELPHI Coll., Contr. Paper 146 to the XXIX ICHEP, Vancouver, 1998;
K. Hamacher, O. Klapp, P. Langefeld, M. Siebel et al., CERN-EP 99/03.
[13] J. B. Gaffney and A.H. Müller, *Nucl. Phys.* B **250**, 501 (1985).
[14] Yu.L.Dokshitzer, V.A.Khoze et al.,*Int. J. Mod. Phys.* A **7**, 1875 (1992).
[15] B.R. Webber, *Phys. Lett.* B **143**, 501 (1984).
[16] I.M. Dremin and V.A. Nechitailo, *Mod. Phys. Lett.* A **9**, 1471 (1994);
I.M. Dremin, *JETP. Lett.* **68**, 559 (1998).